



HAL
open science

Prediction and analytical description of the single laser track geometry in direct laser fabrication from process parameters and energy balance reasoning

Hussam El Cheikh, Bruno Courant, Jean-Yves Hascoët, Ronald Guillén

► To cite this version:

Hussam El Cheikh, Bruno Courant, Jean-Yves Hascoët, Ronald Guillén. Prediction and analytical description of the single laser track geometry in direct laser fabrication from process parameters and energy balance reasoning. *Journal of Materials Processing Technology*, 2012, 212 (9), pp.1832-1839. 10.1016/j.jmatprotec.2012.03.016 . hal-01007191

HAL Id: hal-01007191

<https://hal.science/hal-01007191>

Submitted on 31 Oct 2018

HAL is a multi-disciplinary open access archive for the deposit and dissemination of scientific research documents, whether they are published or not. The documents may come from teaching and research institutions in France or abroad, or from public or private research centers.

L'archive ouverte pluridisciplinaire **HAL**, est destinée au dépôt et à la diffusion de documents scientifiques de niveau recherche, publiés ou non, émanant des établissements d'enseignement et de recherche français ou étrangers, des laboratoires publics ou privés.



Distributed under a Creative Commons Attribution 4.0 International License

Prediction and analytical description of the single laser track geometry in direct laser fabrication from process parameters and energy balance reasoning

H. El Cheikh ^{a,*}, B. Courant ^a, J.-Y. Hascoët ^b, R. Guillén ^a

^a LUNAM Université, GeM (Institut de Recherche en Génie Civil et Mécanique), UMR CNRS 6183, Université de Nantes, Ecole Centrale de Nantes, France

^b Institut de recherche en Communications et en Cybernétique de Nantes (IRCCyN), UMR CNRS 6597, France

Direct laser fabrication (DLF) is a process for the manufacture of functional parts directly from powder injected in a laser beam. Deposition of 316L stainless steel powder on a steel substrate is carried out using a 700 W fiber laser for one module. One problem for this process is the control of the building structure dimensions. In this study a mathematical model implemented in the software Mathematica 8[®] is used to predict the clad cross-section dimensions and obtain an analytical description of the clad geometry. We experimentally notice that the cross-section shape is a disk due to the surface tension forces. Analytical relationships are established between the radius and the center of the disk in one hand and the process parameters in the other hand. This way we show that we can reproduce the laser track geometry in all the area experimentally explored. A number of laser tracks are deposited using a varying process parameter combination in order to compare with our calculation results. This analytical description of the clad geometry could be used in order to improve the calculation quickness of the thermal field induced by the process.

1. Introduction

Since the invention of LASER by Maiman (1960), laser applications growth rapidly and widely in many domains. A variety of industries (automotive, aerospace, navy, defense and many other sectors) use the laser technology for welding, cutting and hardening (Courant et al., 1999). Direct laser fabrication is a strategic application of laser technology based on laser cladding. A powder is injected in a laser beam and fused onto a substrate. The result of the deposition is a clad and the accumulation of those clads allows to fabricate a 3D object from a CAD file. This technique has several advantages over conventional fabrication techniques and can also be combined with subtractive processes as shown by Kerbrat et al. (2010). These advantages include faster processing speed, no requirement of tooling, ability to fabricate complex shapes and retention of a metastable microstructure/composition (Majumdar and Manna, 2003). Meanwhile, one of the disadvantages is the need of more mastery of the deposit laser track geometry (Williams, 2003).

Several works and publications have been developed in the literature to improve and understand the DLF process and the theory of deposition. Wen et al. (2009) present a numerical model which

predicts the coaxial powder flow for the laser direct deposition process, including the particle stream flow in and after the nozzle and laser-particle interaction process. By solving the coupled momentum transfer equations between the particle and gas phase while incorporating particle temperature evolution, the dynamic and thermal behavior of multi-particles in the stream is completely modeled. Partes (2009) study a model which evaluates the catchment efficiency with respect to the molten pool geometry. Its model takes into account the melt pool geometry for low speeds, laser powers and feed rates, and by taking into account the particle melting during the flight for higher speed, laser powers and feed rates. Picasso and Hoadley (1994) developed a 2D, stationary, finite element model to determine the shape of the melt pool in a known clad height by solving a stationary Stefan equation. Picasso et al. (1994) developed a simple geometrical model which allows the determination of the laser beam velocity and the powder feed rate from beam diameter, clad height and powder jet geometry for a specified laser power.

Bamberger et al. (1998) used the Mie theory in a simplified theoretical model to show the influence of the injected particles on laser beam energy transfer to treated surface. Toyserkani et al. (2004) use a transient three-dimensional finite element modeling, to show the effect of laser pulse shaping on the process. This model can predict the clad geometry as a function of time and process parameters including laser pulse shaping, travel velocity, laser pulse energy, powder jet geometry, and material properties. The decrease of the laser beam velocity or the increase of powder feed rate and laser

* Corresponding author at: CRTT, 37 Boulevard de l4 université, BP406, 44602 Saint-Nazaire Cedex, France. Tel.: +33 2 40 17 26 19; fax: +33 2 40 17 26 18.

E-mail address: Hussam-elcheikh@hotmail.fr (H. El Cheikh).

Nomenclature

P	power of laser heat (W)
Q_m	powder feed rate (g/s)
V	velocity of the laser advancement (m/s)
H	height of laser clad (m)
W	width of laser clad (m)
H_f	cross-section height of molten pool (m)
S	cross-section area of laser clad (m ²)
S_f	cross-section area of molten pool (m ²)
R	radius of virtual disk (m)
P_e	powder efficiency
ρ	density (kg/m ³)
Q_l	absorbed laser energy (J/s)
Q_c	heat flow from molten zone to substrate (J/s)
Abs	absorption
T_m	molten temperature (K)
T_0	initial temperature (K)
t	time (s)
α	diffusivity (m ² /s)
d	diameter of spherical molten zone (m)
k	conductivity (W/(mK))
A	area of molten pool (m ²)

pulse energy increases the clad height. Lalas et al. (2007) take into account the process speed and feed rate of the powder to predict the clad characteristics by an analytical approach based on the phenomenon of the surface tension considered as dominant. Onwubolu et al. (2007) investigate the prediction of the geometric form of the clad in laser cladding by powder using response surface methodology and scatter search optimization technique. Oliveira et al. (2005) present a theoretical and experimental study linking the process parameters to geometrical characteristics of an individual laser track using a numerical resolution. Lin and Hwang (2001) suggest a simplified mode function to estimate the clad profiles based on the Gaussian distribution in the jet flow. Liu and Li (2005) presented a model to study the effects of process variables on wall thickness, powder primary efficiency and speed of forming a thin metallic wall in single-pass coaxial laser cladding. The static model of powder mass concentration distribution was defined as a Gaussian function. Either these models give incomplete information or they use the finite element method to calculate the laser track geometry and the induced thermal field and so are very time consuming because of the very small dimensions of the molten bath compare to the building entire part and the very short time of the interaction between one powder grain with the laser beam compare to the time to build the entire part. A way to improve the calculation quickness is to use an analytical description of the surface laser track. In this work, our goal is to propose a pragmatic way to optimize the process linking the laser track geometry to the process parameters, and also to obtain an analytical description of the laser track geometry to improve the thermal calculation quickness. It is shown that it is possible to simulate the shape and the geometrical characteristics of the deposit clad, with an analytical formula, taking into account the process parameters, the width of the clad and the powder efficiency. First it is observed that the cross-section of the clad is always a part of a virtual disk. Then an expression is obtained linking the radius and the center of that disk to the clad width and the powder efficiency.

2. Materials and methods

A coaxial nozzle is used with an IPG Photonics® 700 W fiber laser (150 μ m). A carrier gas (Ar) flow, fixed at 3 L/min, imports the

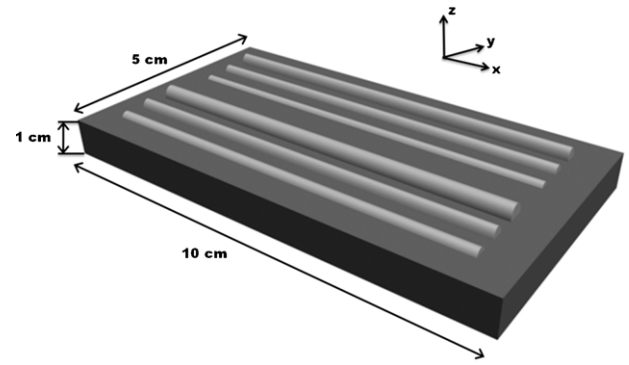


Fig. 1. Substrate dimensions and positions of single laser tracks on the steel substrate.

powder while a secondary gas (Ar) flow, fixed at 5 L/min, is shaping the powder stream. The laser beam is focused on the substrate surface while the distance of work between the nozzle and the focus plan is 5 mm. The beam analysis was carried out with the “FOCUS-MONITOR” from PRIMES GmbH. The laser beam is scanned with a rotation pinhole (about 20 μ m in diameter). This pinhole takes a small part of radiation and 2 mirrors direct the signal to a detector. By scanning the laser beam layer by layer, the laser beam geometry and the spatial distribution of irradiance can be determined. This nozzle is also equipped with a cooling channel to dissipate heat. The focus plan of the powder is beneath the laser at 3.5 mm from the nozzle, the diameter of this focus plan is 0.6 mm.

In this study, powder of 316L stainless steel is used to fabricate the experimental clad. Particles size is between 45 and 75 μ m.

A low carbon steel substrate is used with the dimension mentioned in Fig. 1.

On each substrate, 6 laser tracks are made. In order to avoid any board effect, the 6 laser tracks are carried out at a distance of 10 mm from the substrate boards. The process duration is adjusted in order to obtain always the same length track of 9 cm.

To study effects of the main laser cladding parameters on the clad geometry, tracks are produced in a wide variety of power P (180, 280 and 360 W), velocity V (300, 600 and 900 mm/min) and mass feed rate Q_m (0.025, 0.05 and 0.075 g/s). Samples are polished and etched with Nital (2%). Every combinations of the 3 values of the 3 parameters are explored which represents 27 single tracks. In order to evaluate the accuracy of the experimental results, two cross-sections are made and studied for each of the 27 laser tracks. And for one parameters combination four laser tracks have been made and analyzed. Cross-section characteristics change with the process parameters. Fig. 2 shows for each clad the height (H), the

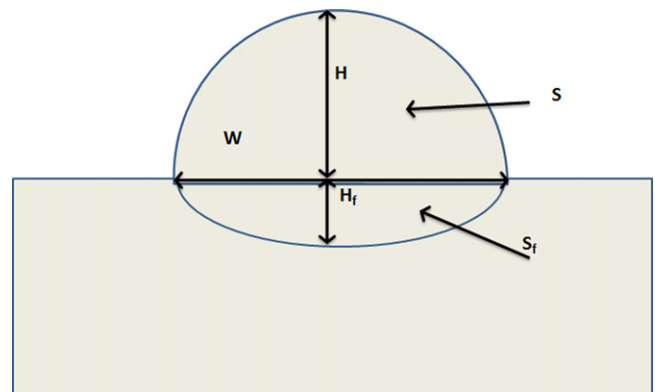


Fig. 2. Cross-section measures for each single laser track.

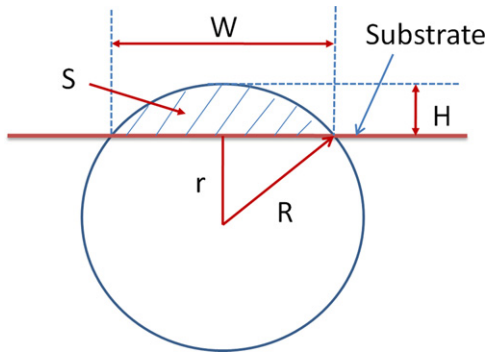


Fig. 3. Schematic of the cross-section.

width (W), the depth penetration (H_f), the area (S) and the penetration area (S_f).

3. Theory

The powder is injected from a coaxial nozzle into the laser, melt and solidify on the substrate.

For a single laser track, the 3 important process parameters are the laser power, the powder feed rate, and the velocity of the laser advancement. These three parameters have a big influence on the clad dimensions.

Actually, we have experimentally observed that if dimensions of the clad depend on the process parameters, the cross-section always remain a part of a virtual disk to which the center can be below or above the work piece surface, so the model uses a circular form to describe the clad cross-section. The disk center is found above the work piece surface when the velocity is not great enough to avoid the accumulation of the deposited material. The usefulness of the proposed model is in one hand to predict the height, the width and the general form and surface of the cross-section in any cases and in the other hand to obtain an analytical description of the clad surface, which then, can be useful to simulate the thermal field induced by the laser heating.

This circular geometry suggests that surface tension forces are dominant. The calculation of the capillary length gives a result of 0.004 m. The liquid bath has a characteristic length smaller than this capillary length and so the gravity effect is negligible and the liquid shape is almost spherical (circular in the cross-section plane and slightly lengthened along the laser displacement axis because of the laser movement).

A similar approach exist, using the Simpson's rule, but is limited to cases where the clad is flattened. It allows describing the clad height and width by Davis et al. (2006), and to optimize the clad parameters by Pinkerton and Li, (2004) and to avoid excessive dilution and overlap porosity by Colaco et al. (1996).

Our approach allows the prediction of the form, the height, the width and the area of the clad from the process parameters.

3.1. Relationships between the geometrical characteristics R , W and the process parameters

Fig. 3 shows the shape of the virtual disk supposed to describe the laser track shape.

The disk is defined by the location of its center and its radius (R). They both depend on the process parameters. W is the clad width and also the chord of the disk at $z=0$. Taking into account only the powder which is incorporated in the clad, the actual surface of the clad cross-section is given by $P_e Q_m / \rho V$.

They are distinguished by the position of the circle center which can be located below or above the substrate surface. The powder

mass deposited is related to the volume of the laser clad above the substrate surface. In the limit case the circle center is located on the substrate surface and one can show that $P_e Q_m / \rho V = \pi R^2 / 2$ and then that the radius of the disk is given by:

$$R = \sqrt{\frac{2P_e Q_m}{\pi \rho V}}$$

This case is a very interesting one to build a structure because of its 1/2 circular geometry.

Outside this limit case:

- Type 1: If $P_e Q_m / \rho V < \pi R^2 / 2$, the center of the disk is below the substrate surface and at a distance $\sqrt{R^2 - (W/2)^2}$ from it. The radius R is obtained by solving the equation:

$$\frac{P_e Q_m}{\rho V} = \frac{1}{6W} \left(R \left(1 - \sqrt{1 - \left(\frac{W}{2R} \right)^2} \right) \times \left(3R^2 \left(1 - \sqrt{1 - \left(\frac{W}{2R} \right)^2} \right) \right) + 4W^2 \right) \quad (1)$$

This case is also interesting and corresponds to the flattened one.

- Type 2: If $P_e Q_m / \rho V > \pi R^2 / 2$, the center of the disk is above the surface substrate and at a distance $\sqrt{R^2 - (W/2)^2}$ from it. The radius R is obtained by solving the equation:

$$\frac{P_e Q_m}{\rho V} = \pi R^2 - \frac{1}{6W} \left(R \left(1 - \sqrt{1 - \left(\frac{W}{2R} \right)^2} \right) \left(3R^2 \left(1 - \sqrt{1 - \left(\frac{W}{2R} \right)^2} \right) \right) + 4W^2 \right) \quad (2)$$

This case cannot be used to build a full density structure but can be interesting for a porous one.

Finally the clad geometry can be expressed as an analytical expression which is the one of the circle of radius R and centered at the distance $\sqrt{R^2 - (W/2)^2}$ below or above the substrate surface. The radius of the disk can be calculated knowing the width (W) and the powder efficiency (P_e). It is to be noticed that the laser power is hidden behind P_e . We suggest two different methods to predict P_e and W .

3.2. Determining P_e and W with parametric relationships

Each clad is defined by the corresponding process parameters (P , Q_m , V). A parametric study is searched linking W and P_e to the process parameters. A relationship as $y = a(P^\alpha Q_m^\beta V^\gamma) + b$ is thus established by El Cheikh et al. (2012), where "y" is one of the laser track geometry parameters while a and b are constants. These relationships are very useful to predict the clad width and height but do not help to understand the physical phenomenon involved during the process. They are used in complement to our theoretical study (Table 1).

3.3. Determining W using a thermal study

The relationship between W and the experimental parameters does not involve the parameter Q_m . This observation shows that a thermal process governs the parameter W . This is also in agreement with the usually accepted fact that only the powder which falls in the melting bath stays in the clad (Lin, 1999). The width of the clad

Table 1
Relationships between the geometrical characteristics of the cross-sections and the process parameters (El Cheikh et al., 2012).

	Combined parameter	R ²
H	$P^{1/4}Q_m^{3/4}/V$	0.944
W	$P^{3/4}V^{1/4}$	0.922
S	$PQ_m/V\sqrt{V}$	0.957
m	$PQ_m/V\sqrt{V}$	0.934
P _e	$P^{3/4}Q_m^{-1/3}V^{-1/2}$	0.910
S _f	$\text{Ln}(P^{4/5}Q_m^{-1/4})$	0.649
H _f	$\text{Ln}(P^2V^{1/4}Q_m^{-1/4})$	0.765

is given by the molten pool dimension. The laser beam moves in the x direction at a constant velocity, many assumptions can be made to simplify the interaction between the laser and the substrate as follow:

1. The substrate is considered as a semi-infinite solid initially at the room temperature T_0 .
2. The molten zone is supposed to be a sphere whose surface is always at the molten temperature T_m .
3. Thermo-physical properties are temperature independent.

In the steady state the pool geometry is constant. An energy balance is established between the absorbed laser energy in unit time, Q_l , and the energy transported through the boundary of the molten pool in contact with the substrate and the deposit clad in unit time Q_c by the heat conduction.

$$Q_l = Q_c \quad (3)$$

The laser energy in unit time absorbed by the work piece is expressed as

$$Q_l = Abs P \quad (4)$$

In these conditions and in case of transient conduction, an analytical solution is given by Holman (1990):

$$Q_c = \frac{kA(T_m - T_0)}{\sqrt{\pi\alpha t}} \quad (5)$$

where A is the surface at the temperature T_m crossed by the heat flux, i.e. the area of the molten pool in contact with the substrate and the deposit clad.

In laser cladding, the melting zone is almost spherical and the surface contact A represents a part of its surface as shown in Fig. 4, $A = f\pi d^2$.

The characteristic time for the passage of the molten zone above a point is given by Liu and Li (2005) as

$$t = \frac{d}{v} \quad (6)$$

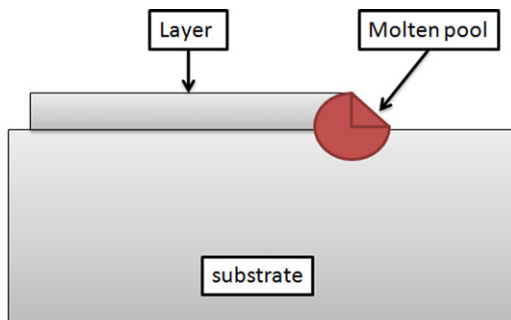


Fig. 4. Schematic view of the spherical molten pool.

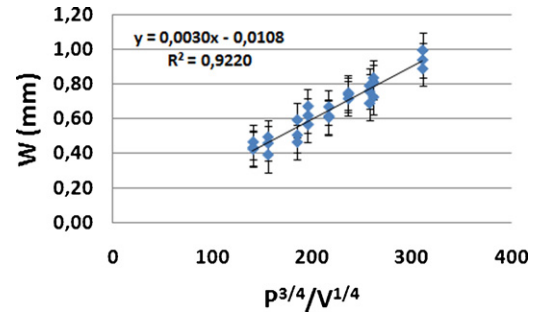


Fig. 5. Width via the combined parameters.

From Eqs. (5) and (6) the diameter of the molten zone is given by

$$d = \left(\frac{Abs}{f}\right)^{2/3} \left(\frac{P\sqrt{\pi\alpha}}{\pi k\sqrt{V}(T_m - T_0)}\right)^{2/3} \quad (7)$$

The width of the molten zone W is approximately equal to this diameter.

The width is given versus the molten temperature and the thermo physical proprieties of the clad material, and depends on the power and the velocity of the laser beam.

4. Results

4.1. Using the parametric relationships

The mathematical model presented above, allows the prediction of the cross-section geometry of the clad, knowing the width and the powder efficiency. The geometrical characteristics of the clad are measured with the aid of a software measuring tools integrated in the optical microscopy system. The width and the powder efficiency are linked to the laser power (P), the powder feed rate (Q_m) and the laser velocity (V) with the following equations:

$$W = 0.0030 \left(\frac{P^{3/4}}{V^{3/4}}\right) - 0.0108 \quad (8)$$

$$P_e = 0.312 \text{Ln} \left(\frac{P^{3/4}}{V^{1/2}Q_m^{1/3}}\right) - 1.995 \quad (9)$$

Figs. 5 and 6 show the relationships between the combined process parameters and the experimental results.

We can now predict the geometrical form of the clad with the proposed mathematical model. This is presented in Fig. 7. The continuous line represents the prediction from the experimental measurements of the width and the powder efficiency. The dashed line is the prediction from the parameters (P, Q_m , V) and the analytical relationships previously determined. It clearly shows that

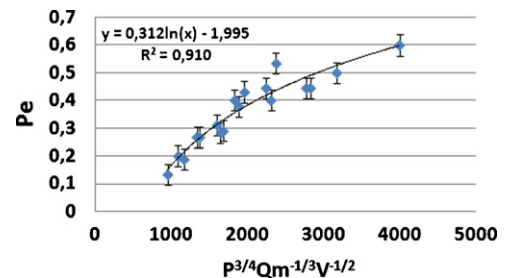


Fig. 6. Power efficiency via the combined process parameters.

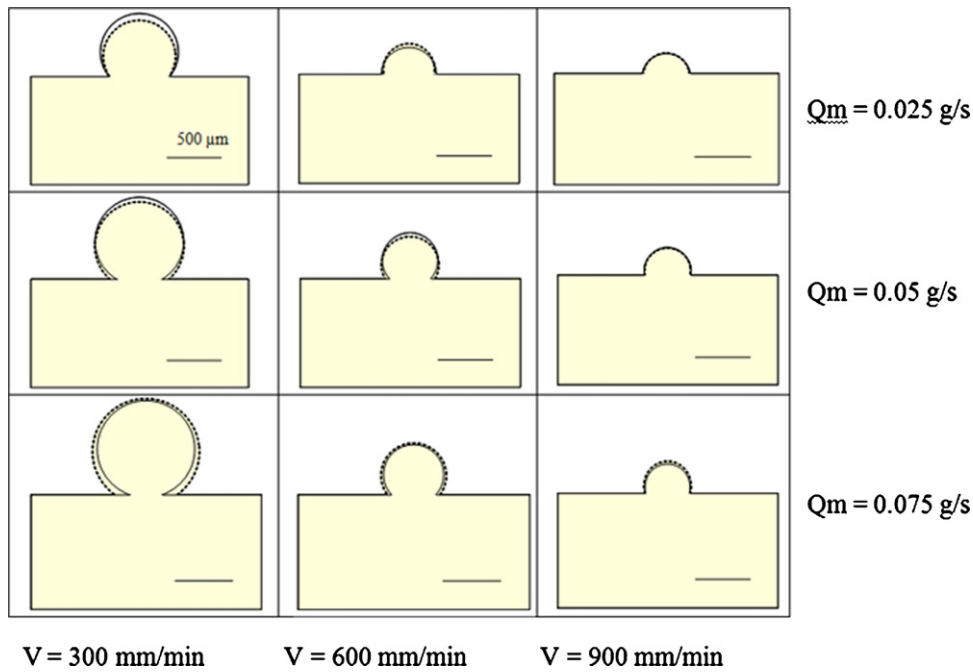


Fig. 7. Confrontation between the geometrical representation of the clad geometry obtained with experimental measures of W and P_e (continuous line) and analytical determination of W and P_e from the parametric relationships (dash line) at $P = 180$ W.

in the limits determined by our experiments we are able to predict the clad geometry from the analytical parametric relationships presented above.

In Fig. 8 the cross-section simulations obtained with the parametric relationships (dashed lines) are compared with those obtained with the experimental measured width (continuous line) and superimposed with the experimental photographs. These overlays are convincing.

4.2. Using the thermal analytical relationships

The thermal analytical model is now used to simulate the cross-section. Results obtained with the analytical model are given in Fig. 9.

The continuous line is the clad representation when W is calculated with the parametric relationships while the dashed line is the clad representation when the width W is calculated from the thermal analytical model.

5. Discussion

We showed in a previous study (El Cheikh et al., 2012) that the laser clad geometrical characteristics are not due to the powder distribution in the powder jet stream but induced by the surface tension forces applied on the melting bath. It is experimentally established that the clad width depends only on the laser power and the laser velocity (Fig. 5). This shows the thermal dependency of the clad width and justifies the analytical thermal modeling of the laser clad width. The powder efficiency depends on the three process parameters through a logarithm function (Fig. 6).

Fig. 8 shows variation of the clad cross-sections with process parameters. Power remaining constant, the laser track height (H) and the cross-section area (S) increase if the velocity decreases or if the powder feed rate increases. For low velocities and high feed rate powder, the powder accumulation leads to the formation of a well

defined cylindrical laser tracks. At the opposite for high velocity and low feed rate powder the clad profile is flattened and matches with a small part of a cylinder. When the laser power increases, the powder efficiency (Fig. 6) and the mass of incorporated powder per meter (g/m) increase.

In our case, the difference between calculated and experimental values always remains under $100 \mu\text{m}$ (results obtained in cases 280 W, 0.025 g/s, whatever is the chosen speed and 180 W, 0.025 g/s, 600 mm/min) and in most cases under $50 \mu\text{m}$ concerning the clad height and the width.

The two suggested ways linking the width to the process parameters are the parametric study or the balance energy reasoning and they lead to very narrow results (Fig. 9). This confirms the validity of the thermal model. Only a parametric study seems to be able to link the powder efficiency and the process parameters. However, the powder efficiency depends on the particular nozzle used and seems difficult to generalize with an analytical relationship. Partes (2009) proposed an analytical model of the catchment efficiency in which powder grains are incorporated if they fall in the melting bath and/or if they melt during the flight. The model depends on the melting bath geometry measured with a good thermal camera or difficult to simulate without the time consuming finite element method. And as authors say "toward higher melt pool lengths the difference between experiment and calculation of the catchment efficiency was strongly increasing". An analytical formula proposed by Liu and Li (2005) has been tried with our experimental results but this has not been successful. A simple and predictive analytical model for the powder efficiency catchment remains to be done. So P_e is kept as an experimental entry in this model. The model proposed in this work, can predict the general geometry of the clad cross-section. This model is particularly interesting because it allows the width prediction of the clad layer analytically.

$$W = K \left(\frac{P\sqrt{\pi\alpha}}{\pi k\sqrt{V}(T_m - T_0)} \right)^{2/3}$$

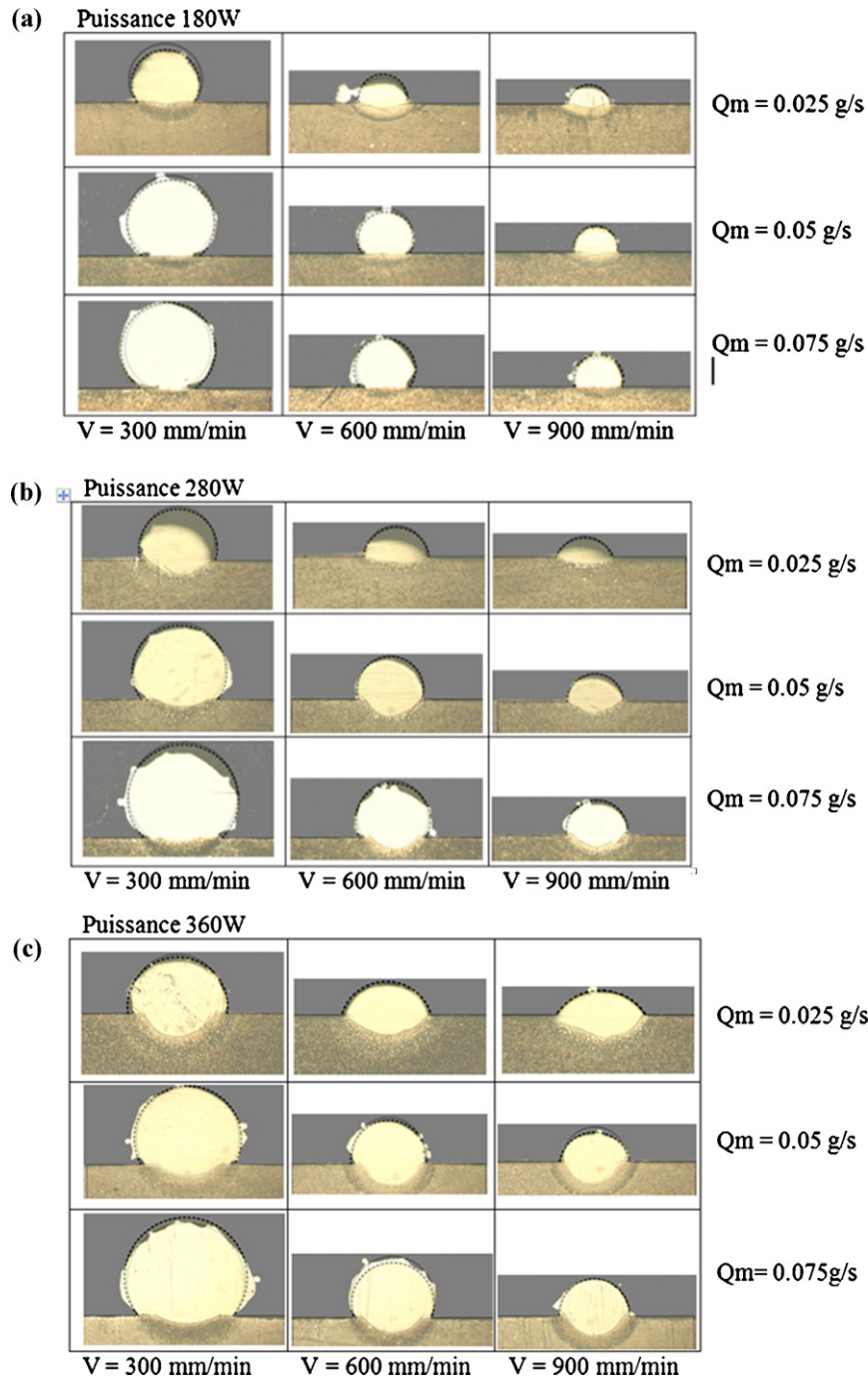


Fig. 8. Confrontation between experimental results and simulated ones obtained with the analytical relationships at different power: (a) 180 W, (b) 280 W and (c) 360 W.

The width depends on laser power, velocity of advancement, material properties as the conductivity, the diffusivity and the molten temperature. The constant K depends on the interaction between the laser beam and the material with the absorption coefficient and from the surface fraction of the melt pool through which the heat flows in the material. In our case, these good results are obtained with a constant K equal to 0.26. Independently of the used model the absorption coefficient has to be experimentally measured. This is particularly true concerning the direct laser fabrication process with coaxial powder injection because of the complex interaction process between the material and the laser

beam. Few experimental trials have to be done in order to adjust the model whatever it is. These few experiments can be used to determine the K constant and the relationship between P_e and the experimental parameters. This model can then be used to optimize the process parameters for one particular application. Choosing the width W and the radius R , one can find the process parameters P , Q_m and V . The validity domain of this model is limited by the chosen extreme values of the experimental parameters P , Q_m and V . One can choose a larger domain than our but must find a good relationship between P_e and the process parameters P , Q_m and V . The thermal model assumptions are not restrictive.

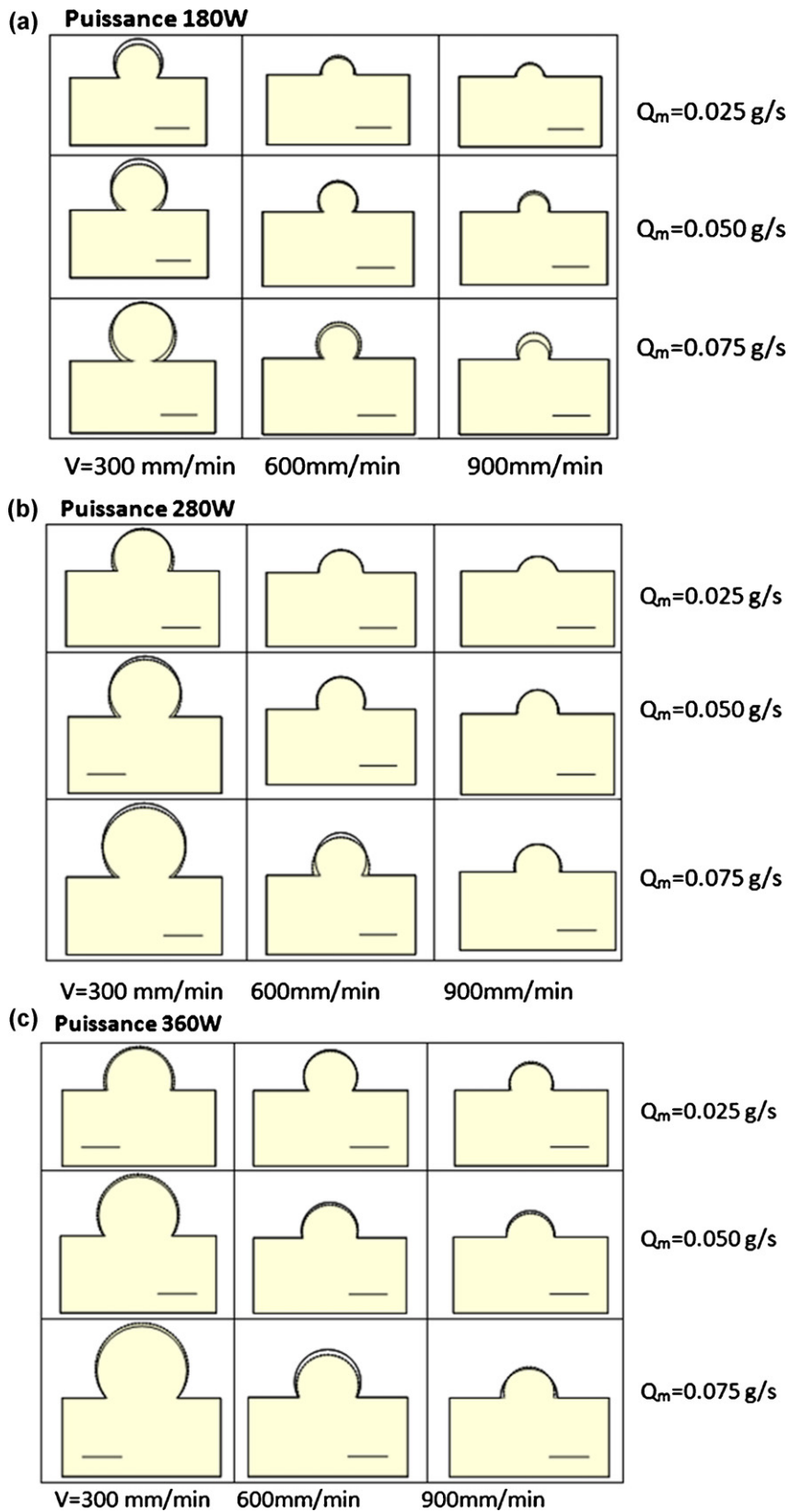


Fig. 9. Confrontation between the geometrical representation of the clad geometry obtained with the analytical relationships (continuous line) and with the thermal analytical model (dash line) at different power: (a) 180 W, (b) 280W and (c) 360W.

6. Conclusion

Laser cladding process success depends on the ability to predict the laser clad geometry (form and dimensions) from the process parameters. Acting the fact that the laser clad cross-section looks like a disk we have related the circle center position and the circle diameter to the clad width W and the powder efficiency P_e . Two ways are explored to calculate W from the process parameters. Finally the cross-section simulations are compared to the experimental photographs. These overlays are convincing and so this modeling is able to predict the complete clad geometry with an analytical expression.

Assuming the fact that the clad geometry is governed by the surface tension on the melted bath and so that the clad geometry is a part of a disk it is shown that it is possible to predict, with a good uncertainty, the complete geometrical characteristics of laser clad. The other interest point of this model is that this analytical formula can help in a thermal study to determine the shape of the molten pool, and the distribution of temperature in the piece.

References

- Bamberger, M., Kaplan, W.D., Medres, B., Shepeleva, L., 1998. Calculation of process parameters for laser alloying and cladding. *Journal of Laser Applications* 10 (1), 29–33.
- Colaco, R., Costa, L., Guerra, R., Villar, R., 1996. A simple correlation between the geometry of laser cladding tracks and the process parameters. *Laser processing: surface treatment and film deposition*. In: Mazumder, J., Conde, O., Villar, R., Steen, W. (Eds.), Series E: Appl. Sciences, vol. 307.
- Courant, B., Hantzpergue, J.J., Benayoun, S., 1999. Surface treatment of titanium by laser irradiation to improve resistance to dry-sliding friction. *Wear* 236 (1–2), 39–46.
- Davis, S.J., Watkins, K.G., Deardean, G., Fearon, F., Zeng, J., 2006. Optimum deposition parameters for the direct laser fabrication (DLF) of quasi-hollow structures. In: *Photon Conference Manchester, OPD*: 13.14.
- El Cheikh, H., Courant, B., Samuel, B., Hascoët, J.Y., Guillén, R., 2012. Analysis and prediction of single laser tracks geometrical characteristics in coaxial laser cladding process. *Optics and Lasers in Engineering* 50, 413–422.
- Holman, J.P., 1990. *Heat Transfer*, 7th ed. p. 145.
- Kerbrat, O., Mognol, P., Hascoët, J.-Y., 2010. Manufacturability analysis to combine additive and subtractive processes. *Rapid Prototype Journal* 16 (1), 63–72.
- Lalas, C., Tsirbas, K., Salonitis, K., Chryssoulouris, G., 2007. An analytical model of the laser clad geometry. *International Journal of Advanced Manufacturing Technology* 32, 34–41.
- Lin, J., 1999. A simple model of powder catchment in coaxial laser cladding. *Optics and Laser Technology* 31, 233–238.
- Lin, J., Hwang, B.C., 2001. Clad profiles in edge welding using a coaxial powder filler nozzle. *Optics and Laser Technology* 33, 267–275.
- Liu, J., Li, L., 2005. Effects of powder concentration distribution on fabrication of thin-wall parts in coaxial laser cladding. *Optics and Laser Technology* 37, 478–482.
- Maiman, T.H., 1960. Stimulated optical radiation in ruby. *Nature* 187, 493–494.
- Majumdar, J.D., Manna, I., 2003. *Laser processing of materials*. Sadhana 28, 495–562.
- De Oliveira, U., Ocelik, V., De Hosson, J.Th.M., 2005. Analysis of coaxial laser cladding processing conditions. *Surface & Coatings Technology* 197, 127–136.
- Onwubolu, G.C., Davim, J.P., Oliveira, C., Cardoso, A., 2007. Prediction of clad angle in laser cladding by powder using response surface methodology and scatter search. *Optics and Laser Technology* 39, 1130–1134.
- Partes, K., 2009. Analytical model of the catchment efficiency in high speed laser cladding. *Surface and Coatings Technology* 204, 366–371.
- Picasso, Hoadley, M., 1994. Finite element simulation of laser surface treatments including convection in the melt pool. *International Journal of Numerical Methods for Heat & Fluid Flow* 4, 61–83.
- Picasso, M., Marsden, C.F., Wagniere, J.D., Frenk, A., Rappaz, M., 1994. A simple but realistic model for laser cladding. *Metallurgical and Materials Transactions B-Process Metallurgy and Materials Processing Science* 25, 281–291.
- Pinkerton, A.J., Li, L., 2004. Modelling the geometry of a moving laser melt pool and deposition track via energy and mass balances. *Journal of Applied Physics D: Applied Physics* 37, 1885–1895.
- Toyserkani, E., Khajepour, A., Corbin, S., 2004. 3-D finite element modeling of laser cladding by powder injection: effects of laser pulse shaping on the process. *Optics and Lasers in Engineering* 41, 849–869.
- Wen, S.Y., Shin, Y.C., Murthy, J.Y., Sojka, P.E., 2009. Modeling of coaxial powder flow for the laser direct deposition process. *International Journal of Heat and Mass Transfer* 52, 5867–5877.
- Williams, C.B., 2003. *Structural–Property Relationships in Materials – ME 6796*. Georgia Institute of Technology, Atlanta, GA.